Influence of water matrix species on persulfate oxidation of phenol: reaction kinetics and formation of undesired degradation byproducts

Jie Ma, Haiyan Li, Yongqi Yang and Xuening Li

ABSTRACT

The present study explored the influence of Cl^-, Br^-, CO_3^{2-}, HCO_3^-, PO_4^{3-}, HPO_4^{2-}, NO_3^-, SO_3^{2-} and natural organic matter (NOM) on the reaction kinetics and the formation of undesired degradation byproducts during phenol oxidation by heat-activated persulfate (PS). CO_3^{2-} and PO_4^{3-} promoted the phenol degradation, because the hydrolysis of CO_3^{2-} and PO_4^{3-} created basic pH conditions which were conducive to enhanced PS oxidation rate. Br^- promoted the reaction by reacting with sulfate radicals ($SO_4^{\bullet-}$) to produce bromine radicals that can selectively react with electron-rich phenol. NOM scavenged reactive $SO_4^{\bullet-}$, thus inhibiting the reaction. As a strong reducing agent, SO_3^{2-} rapidly reduced PS, thus completely suppressing the reaction. HCO_3^-, HPO_4^{2-}, Cl^-, and NO_3^- had negligible impact on PS oxidation of phenol. Six intermediates were detected in the no anion control using gas chromatography–mass spectrometry (GC-MS). Various toxic halogenated phenols and halogenated hydroquinones were detected in the treatment containing Cl^- and Br^-. In contrast, in the treatment containing CO_3^{2-}, HCO_3^-, PO_4^{3-}, HPO_4^{2-}, and NO_3^-, no new intermediates were identified except for the intermediates already detected in the control treatment. Based on intermediates identified, reaction pathways for PS oxidation of phenol without anions and in the presence of halides were proposed respectively.

Key words | degradation intermediate, disinfection, humic acids, inorganic ions, matrix constituents, peroxydisulfate

Jie Ma (corresponding author)
Haiyan Li
Yongqi Yang
State Key Laboratory of Petroleum Pollution Control,
China University of Petroleum-Beijing,
Beijing 102200,
China
E-mail: *rubpmj@sina.com*

Xuening Li
State Key Laboratory of Petroleum Pollution Control,
CNPC Research Institute of Safety & Environment Technology,
Beijing 102206,
China

NOMENCLATURE

PS	Persulfate
PS-AOP	Persulfate-based advanced oxidation process
SR-AOP	Sulfate radical-based advanced oxidation process
NOM	Natural organic matter
GC-MS	gas chromatography–mass spectrometry

INTRODUCTION

As a novel and powerful oxidant, persulfate ($S_2O_8^{2-}$) ($E_0 = 2.01$ V) has recently been increasingly used for soil and groundwater remediation and water treatment. The persulfate (PS) ion has a O–O bond with a bond distance of 1.453 Å and a bond energy of 140 kJ/mol (Zhang *et al.* 2015). After activation, the O–O bond would break to generate the sulfate radical ($SO_4^{\bullet-}$), which is an even more powerful oxidant ($E_0 = 2.60$ V) that can rapidly oxidize most refractory organic pollutants in water (Sun & Wang 2015). Keeping a high abundance of $SO_4^{\bullet-}$ is critical for the successful application of a persulfate-based advanced oxidation process (PS-AOP) (Hu & Long 2016). However, naturally occurring inorganic anions and natural organic matter (NOM) that are ubiquitous in waters may scavenge reactive radicals and reduce the efficiency of PS-AOP (Ma *et al.* 2018). Successful application of PS-AOP requires improved understanding of the influence of these scavenging matrix species.

Several studies explored the impacts of matrix species on the kinetics of PS-AOP (Bennedsen *et al.* 2012; Jiang *et al.* 2016; Luo *et al.* 2016; Ma *et al.* 2018). However, most of these studies only investigated three to five matrix species

doi: 10.2166/wst.2018.147

among which Cl^-, CO_3^{2-}/HCO_3^-, and NOM received the most attention. The chemical compositions of aquatic environments are very complex and may contain various types and abundance of inorganic and organic matrix constituents. A more inclusive study that investigated more matrix species would be of great value for a deeper and more comprehensive understanding of this problem. This knowledge would help practitioners to identify the conditions where PS-AOP may or may not be applicable and estimate the dosage requirement of the oxidant.

Phenolic compounds are a group of high production-volume chemicals that find broad applications in various industrial processes and are a ubiquitous class of environmental contaminants commonly detected in various aquatic and terrestrial environments (Anipsitakis *et al.* 2006). Phenols and their derivatives are corrosive to the eyes, skin, and respiratory tract and causes harmful effects on the central nervous system and heart, thereby producing dysrhythmia, seizures, and persistent vegetative state in affected persons (Anipsitakis *et al.* 2006). Eleven phenolic compounds have been classified as priority pollutants by USEPA (Anipsitakis *et al.* 2006). Moreover, phenols are the main configurations composed of humic substances, which are regarded as the important NOM in the environment. Therefore, phenol is often invoked as a model for phenolic moieties in NOM (Liu *et al.* 2015).

Various studies have explored the effectiveness of PS-AOP by different activation methods in degrading phenols (Anipsitakis *et al.* 2006; Ahmad *et al.* 2013; Ma *et al.* 2017). However, the impacts of water matrix species on PS oxidation of phenols are not well understood. In addition, because of the electron donating capacity of the hydroxyl group, phenols are especially susceptible to electrophilic substitution reactions with electrophiles. Previous studies demonstrated that reactions between halide anions and $SO_4^{\bullet-}$ may generate reactive halogen radicals including $X^{\bullet}$, $X_2^{\bullet-}$, and $XOH^{\bullet-}$. These secondary radicals are electrophilic species that can react with phenols to form toxic halogenated byproducts (Anipsitakis *et al.* 2006; Liu *et al.* 2015). Besides halides, little is currently known about the influence of anions other than halides on the formation of undesired degradation byproducts during PS-AOP. It is not known whether the presence of anions such as $CO_3^{2-}/HCO_3^-/NO_3^-$ may also lead to the formation of undesired degradation byproducts. A comprehensive study that investigates the impacts of anions other than halides would help to fill this important knowledge gap.

This is the first study that has a comprehensive investigation of the impacts of eight anions (CO_3^{2-}, HCO_3^-, Cl^-, Br^-, PO_4^{3-}, HPO_4^{2-}, NO_3^-, and SO_3^{2-}) and NOM on the reaction kinetics and the formation of undesired degradation byproducts during phenol oxidation by sulfate radical-based advanced oxidation process (SR-AOP). Formation of degradation byproducts was identified using gas chromatography–mass spectrometry (GC-MS).

MATERIALS AND METHODS

Chemicals

Phenol was purchased from Tianjin Yongda Chemical Regent Company (Tianjin, China). $K_3PO_4{\cdot}3H_2O$ (>99%) was purchased from Tianjin Fuchen Chemical Reagent Works (Tianjin, China). H_2SO_4 (95–98%) and $NaNO_3$ (>98%) were purchased from Beijing Chemical Reagent Works (Beijing, China). $Na_2S_2O_8$ (>99%), NaCl (>99%), NaBr (>99%), KH_2PO_4 (>99.5%), $NaHCO_3$ (>99.8%), Na_2CO_3 (>99.8%) and Na_2SO_3 (>98.0%) were purchased from Aladdin BioChem Technology (Shanghai, China). Methanol (>99.9%) and dichloromethane were purchased from Fisher Scientific. Humic acid (HA, ash ≤10%) was purchased from Sinopharm Chemical Reagent Beijing (Beijing, China). The reaction solution was prepared using ultrapure water (18.2 MΩ cm) produced by a Master-RUV ultrapure water system (Hitech Instruments, Shanghai, China).

Experimental procedure

In order to explore the influence of matrix species on phenol degradation, batch experiments were conducted in 50 mL solution that contained 10 mM PS, 0.1 mM phenol and one type of matrix species in each experiment. Eight anions (CO_3^{2-}, HCO_3^-, Cl^-, Br^-, PO_4^{3-}, HPO_4^{2-}, NO_3^-, and SO_3^{2-}) and NOM (humic acid) were investigated. Three anion concentrations (1 mM, 10 mM, and 100 mM) and four NOM concentrations (11.6, 23.1, 61.7, and 123.4 mg/L-TOC) were explored. No pH buffer was used in order to avoid potential interference from reactions among buffering species, PS, phenol and matrix species. All degradation experiments were conducted in triplicates at 50 °C in a constant-temperature water bath shaker (HWS-24, Shanghai Yiheng, China). The results were reported as the average value with standard deviation. Whether differences between treatments were statistically significant was determined using Student's *t*-test at the 95% confidence level.

Sample collection and analysis

At predetermined sampling time, 1 mL reaction solution was collected and quenched with 0.02 mL Na_2SO_3 (1 M) immediately. A high pressure liquid chromatography (Agilent 1260 Infinity, USA) equipped with a diode array detector (DAD) and a reversed-phase Poroshell 120 EC-C18 analytical column (100 mm × 4.6 mm × 2.7 μm) were used for phenol analysis. The detection wavelength of DAD was 270 nm. The injection volume was 10 μL. A mixture of 70% methanol and 30% water was used as the mobile phase at a flow rate of 1 mL/min. The temperature of the column was set at 30 °C. A pH meter (Rex DZS-708, Shanghai INESA Scientific Instrument, China) was used to measure the solution pH at the beginning and at the end of each degradation experiment.

Reaction intermediates and pathways

In order to identify the degradation byproducts during PS oxidation of phenol, batch experiments were conducted in 50 mL solution that contained 5 mM phenol, 20 mM PS, and 200 mM selected anions (CO_3^{2-}, HCO_3^-, Cl^-, Br^-, PO_4^{3-}, HPO_4^{2-}, and NO_3^-) as well as in the absence of anions (control treatment). At the desired sampling times during the experiment, a 10 ml water sample was collected and adjusted to pH < 1 with sulfuric acid. Then the water sample was extracted with 1 mL dichloromethane. The dichloromethane extracts collected at different sampling times were combined and then analyzed by GC-MS (Agilent 7890-5977B, USA) equipped with an HP-5 fused silica capillary column (30 m × 0.53 mm × 1.5 μm). The carrier gas was helium (99.999%) with a flow rate of 1.5 mL/min. The temperature program was as follows: initial temperature of 40 °C held for 10 min, then increased at a rate of 10 °C/min to 300 °C, and held for 10 min. The injector temperature was 200 °C. The transfer line temperature was 250 °C. The mass detector was set at the following conditions: operated in the standard electron ionization (EI) mode of 70 eV in the 50–400 amu scan range; the ion source temperature was 230 °C; and the quadrupole temperature was 150 °C.

RESULTS AND DISCUSSION

Impacts of Cl^- on reaction kinetics

Cl^- did not affect the PS oxidation of phenol. The phenol degradation plots of 1 mM, 10 mM, and 100 mM of Cl^- almost overlapped with the plot of the no anion control (Figure 1(a)). The phenol concentration data can be fitted by the first-order kinetic model to calculate the pseudo-first-order degradation rate constant (k_{obs}). The k_{obs} of 1–100 mM of Cl^- had no statistically significant difference ($p > 0.05$) from that of the control (Figure 2(a)). The phenol removal efficiency data support the k_{obs} data (Figure 2(b)). Reactions of Cl^- with $SO_4^{\bullet-}$ produce chlorine radicals ($Cl^\bullet$ and $Cl_2^{\bullet-}$ and $ClOH^{\bullet-}$ in Equations (1)–(4)). Chlorine radicals are very reactive with electron rich compounds such as phenol. For example, the reaction rate of $Cl_2^{\bullet-}$ with phenol is as high as $4.0 \times 10^8\ M^{-1}{\cdot}s^{-1}$. The high reactivity of secondary chlorine radicals with phenol offset the inhibitory effects due to $SO_4^{\bullet-}$ scavenging by Cl^-, therefore phenol

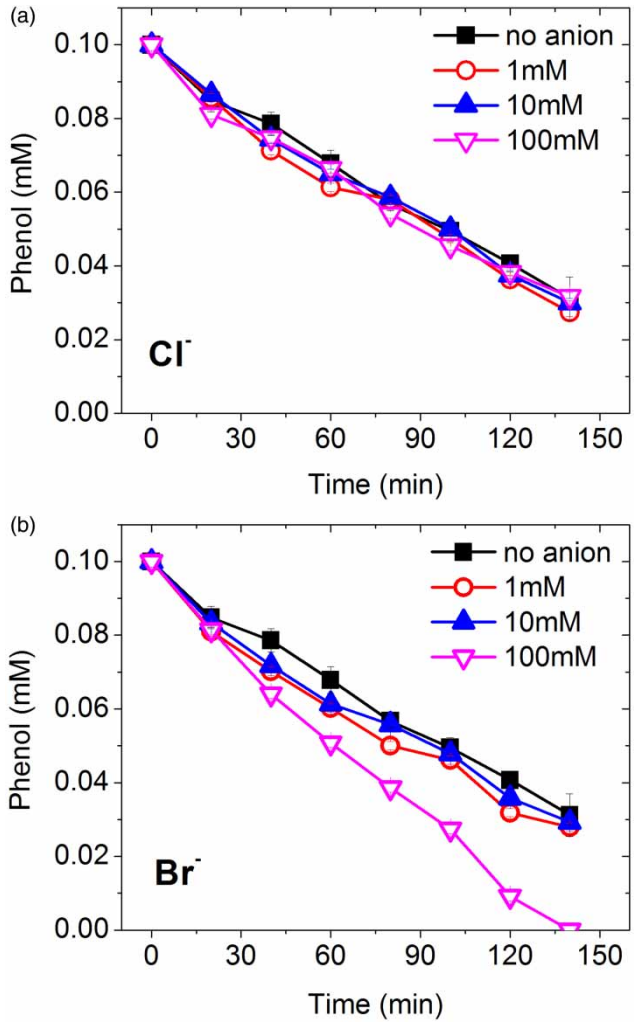

Figure 1 | Impacts of Cl^- and Br^- on phenol oxidation by TAP. Experimental conditions: $[PS]_0 = 10$ mM, | [Phenol] = 0.1 mM, and T = 50 °C.

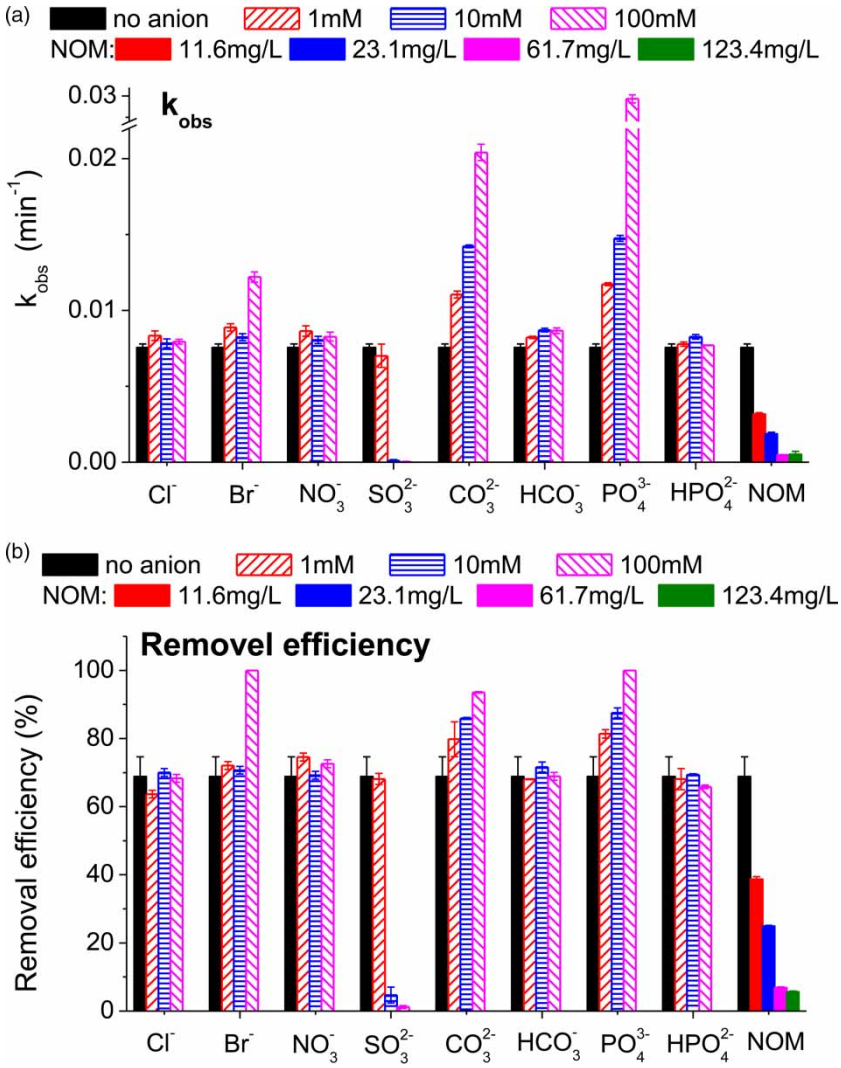

Figure 2 | First-order degradation rate constant of phenol (k_{obs}) and phenol removal efficiency after 140 min of reaction in the presence of different matrix species.

degradation was not affected by the presence of up to 100 mM of Cl^-.

$$SO_4^{\bullet-} + Cl^- = SO_4^{2-} + Cl^{\bullet} \quad k = 3.0 \times 10^8\ M^{-1} \cdot s^{-1} \tag{1}$$

$$Cl^{\bullet} + Cl^- = Cl_2^{\bullet-} \quad k = 8.5 \times 10^9\ M^{-1} \cdot s^{-1} \tag{2}$$

$$H_2O + Cl^{\bullet} = ClOH^{\bullet-} + H^+ \quad k = 1.3 \times 10^3\ M^{-1} \cdot s^{-1} \tag{3}$$

$$H_2O + Cl_2^{\bullet-} = ClOH^{\bullet-} + H^+ + Cl^- \quad k_{[H_2O]} = 100 \cdot s^{-1} \tag{4}$$

Impacts of Br^- on reaction kinetics

Br^- of 100 mM significantly ($p < 0.05$) promoted the phenol degradation while the promoting effects was insignificant ($p > 0.05$) for 1–10 mM of Br^- (Figure 1(b)). The influence of Br^- on the kinetics of SR-AOP is rarely studied. A few available studies reported conflicting results. Wang *et al.* found that 500 mM of Br^- promoted the bleaching of azo dye Orange II by Co^{2+}/PMS (Wang *et al.* 2011). De Luca *et al.* found that Br^- promoted the degradation and mineralization of nitrobenzene by UV/PS/Fe^{2+} while inhibiting the degradation of benzophenone-4, nitrobenzoic acid, atrazine, and ampicillin (De Luca *et al.* 2017). Yang *et al.* investigated

UV/PS degradation of a mixture of benzoic acid (BA), 3-cyclohexene-1-carboxylic acid (3CCA) and cyclohexanecarboxylic acid (CCA) and found that Br^- inhibited the degradation of BA and CCA but did not affect the degradation of 3CCA (Yang *et al.* 2014). In our previous study, we investigated impacts of Br^- on the oxidation of a mixture of benzene, toluene, ethylbenzene, and xylenes (BTEX) by heat-activated PS (Ma *et al.* 2018). It was found that Br^- completely suppressed the degradation of benzene while 500 mM of Br^- strongly promoted the degradation of three xylene isomers. Br^- scavenges $SO_4^{\bullet-}$ to produce $Br^\bullet$, which further reacts with Br^- and OH^- to produce bromine radicals ($Br^\bullet$, $Br_2^{\bullet-}$, and $BrOH^\bullet$) (Equations (5)–(7)). Although these reactions consume reactive $SO_4^{\bullet-}$, the produced bromine radicals can selectively react with electron-rich phenol, thus the overall degradation rate was increased.

$$SO_4^{\bullet-} + Br^- = SO_4^{2-} + Br^\bullet \quad k = 3.5 \times 10^9\ M^{-1} \cdot s^{-1} \tag{5}$$

$$Br^\bullet + Br^- = Br_2^{\bullet-} \quad k = 1.0 \times 10^{10}\ M^{-1} \cdot s^{-1} \tag{6}$$

$$OH^- + Br^\bullet = BrOH^{\bullet-} \quad k = 1.3 \times 10^{10}\ M^{-1} \cdot s^{-1} \tag{7}$$

Impacts of NO_3^- on reaction kinetics

NO_3^- did not affect the phenol oxidation by PS. The phenol degradation plots of 1 mM, 10 mM, and 100 mM of NO_3^- overlapped with that of the no anion control (Figure 3(a)). The negligible impacts of NO_3^- on SR-AOP have also been reported by other studies (Yang *et al.* 2010; He *et al.* 2014; Ma *et al.* 2018). Theoretically, NO_3^- can scavenge $SO_4^{\bullet-}$ to produce less reactive $NO_3^\bullet$ (Equation (8)). However, this reaction is very slow with a rate constant of 5.5×10^4 $M^{-1}\,s^{-1}$. Therefore, the scavenging effect of NO_3^- can be neglected.

$$SO_4^{\bullet-} + NO_3^- = SO_4^{2-} + NO_3^\bullet \quad k = 5.5 \times 10^4\ M^{-1}\,s^{-1} \tag{8}$$

Impacts of SO_3^{2-} on reaction kinetics

SO_3^{2-} significantly inhibited the PS oxidation of phenol. Phenol degradation was significantly delayed in the presence of 1 mM SO_3^{2-}, and 10–100 mM of SO_3^{2-} completely suppressed phenol degradation (Figure 3(b)). As a strong reducing agent, SO_3^{2-} rapidly quenches PS to form SO_4^{2-}. Based on the reaction stoichiometry, 1 mole SO_3^{2-} can consume 1 mole PS. Therefore, theoretically, 1 mM SO_3^{2-} could only consume 10% of 10 mM PS. In the treatment containing 1 mM SO_3^{2-}, the phenol concentration did not change during the first 40 min of reaction (Figure 3(b)). After 40 min, SO_3^{2-} was depleted by PS, and excessive PS can continue to oxidize phenol. Therefore, phenol concentration began decreasing after 40 min. In contrast, phenol degradation was completely suppressed in the presence of $\geq$10 mM SO_3^{2-}. In fact, sodium sulfite is routinely used as a quenching agent to terminate the reaction between $SO_4^{\bullet-}$ and organic compounds in laboratory studies (Ma *et al.* 2018).

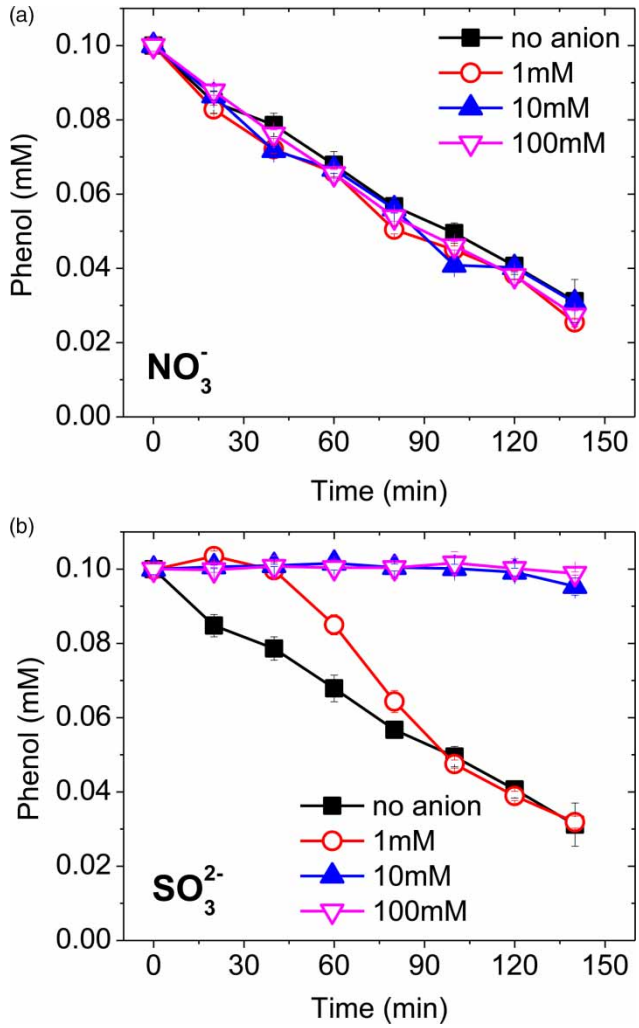

Figure 3 | Impacts of NO_3^- and SO_3^{2-} on phenol oxidation by TAP. Experimental conditions: $[PS]_0 = 10$ mM, [Phenol] = 0.1 mM, and T = 50 °C.

$$SO_3^{2-} + S_2O_8^{2-} = 3SO_4^{2-} + 2H^+ \tag{9}$$

Impacts of CO_3^{2-} on reaction kinetics

CO_3^{2-} promoted the PS oxidation of phenol, and the promoting effect was enhanced with increasing CO_3^{2-} concentration (Figure 4(a)). The k_{obs} of 1 mM, 10 mM and 100 mM of CO_3^{2-} were 1.5, 1.9 and 2.7 times higher than that of the no anion control (Figure 2(a)). After 140 min of oxidation, the phenol removal efficiencies of 1 mM, 10 mM and 100 mM of CO_3^{2-} were 79.8± 5.1%, 86.0 ± 0.3% and 93.5 ± 0.2% which were all significantly higher ($p < 0.05$) than that of the control (68.8 ± 5.8%) (Figure 2(b)).

CO_3^{2-} are usually considered to be $SO_4^{\bullet-}$ scavengers that transform $SO_4^{\bullet-}$ to less reactive carbonate radical ($CO_3^{\bullet-}$) through Equation (10). However, several studies show that $CO_3^{\bullet-}$ can selectively participate in the oxidation of the electron rich compounds (Yang *et al.* 2014). Phenol is a typical electron rich compound, thus $CO_3^{\bullet-}$ can effectively oxidize phenol. Another positive effect of CO_3^{2-} is that the hydrolysis of CO_3^{2-} creates a basic-pH condition (Table 1). Phenol degradation by PS was significantly promoted by the basic pH, which can be attributed to three reasons (Ma *et al.* 2017). The first one is that the base activates PS and increases its oxidation power (Furman *et al.* 2010). The second reason is that basic pH enhanced the reactivity of phenol. Phenol exists in the anionic form (called phenoxide) when the solution pH is higher than 10. Compared to phenol, phenoxide is one to seven orders of magnitude more reactive with common oxidizing radicals (Neta *et al.* 1988). Therefore, basic pH transforms less reactive phenol to more reactive phenoxide, thus increasing the overall reaction rate. The third reason is that phenoxide can activate PS while phenol can not. Ahmad *et al.* reported that phenol (pK_a of 10.0) can activate persulfate at pH 12 but not at pH 8, since activation occurred only via the phenoxide form (Ahmad *et al.* 2013). Overall, CO_3^{2-} has both negative effects (scavenging reactive $SO_4^{\bullet-}$) and positive effects (creating basic pH conditions and selectively reacting with electron-rich phenol) on PS degradation of phenol. Our results suggest that the positive effects dominated over the negative ones and thus the phenol degradation was significantly promoted by increasing CO_3^{2-} concentrations.

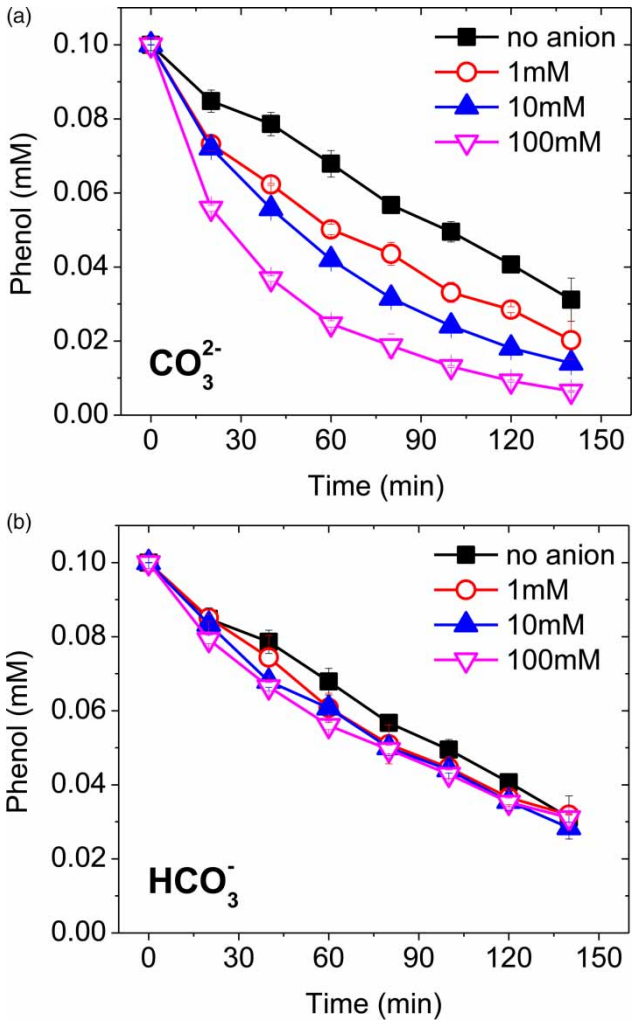

Figure 4 | Impacts of CO_3^{2-} and HCO_3^- on phenol oxidation by TAP. Experimental conditions: $[PS]_0 = 10$ mM, [Phenol] = 0.1 mM, and T = 50 °C.

$$SO_4^{\bullet-} + CO_3^{2-} = SO_4^{2-} + CO_3^{\bullet-} \quad k = 6.1 \times 10^6\ M^{-1}\ s^{-1} \tag{10}$$

Impacts of HCO_3^- on reaction kinetics

HCO_3^- did not affect the PS oxidation of phenol. The phenol degradation plots in the presence of 1 mM, 10 mM and 100 mM of HCO_3^- almost overlapped with that of the no anion control (Figure 4(b)). Conflicting results are reported on the influence of HCO_3^- on SR-AOP. Many studies report that HCO_3^- reduces the contaminant oxidation rate by reacting with reactive $SO_4^{\bullet-}$ to form less reactive bicarbonate radicals ($HCO_3^{\bullet}$) (Equation (11)) (Nie *et al.* 2014; Luo *et al.* 2016; Yang *et al.* 2017). However, several recent studies demonstrate that $HCO_3^{\bullet}$ selectively oxidizes electron rich compounds with relatively fast rate (Yang *et al.* 2014). Since phenol is an electron rich compound, the high reaction rate of $HCO_3^{\bullet}$ with phenol may offset the negative effects due to $SO_4^{\bullet-}$ scavenging, therefore HCO_3^- does not affect phenol

Table 1 | Changes in pH at the beginning and at the end of each degradation experiment

Inorganic anions

	1 mM		10 mM		100 mM	
	$pH_{initial}$	pH_{final}	$pH_{initial}$	pH_{final}	$pH_{initial}$	pH_{final}
Na_2CO_3	10.3 ± 0.2	9.6 ± 0.3	10.9 ± 0.3	10.7 ± 0.3	11.5 ± 0.2	11.3 ± 0.2
$NaHCO_3$	9.0 ± 0.1	7.4 ± 0.2	9.5 ± 0.2	9.2 ± 0.3	9.8 ± 0.2	9.5 ± 0.2
$NaNO_3$	4.1 ± 0.3	3.6 ± 0.2	4.2 ± 0.1	3.6 ± 0.2	6.1 ± 0.2	3.9 ± 0.1
KCl	4.4 ± 0.2	3.6 ± 0.1	4.3 ± 0.2	3.6 ± 0.1	3.9 ± 0.1	3.5 ± 0.1
NaBr	4.3 ± 0.1	3.6 ± 0.0	4.5 ± 0.2	3.6 ± 0.1	6.3 ± 0.3	4.2 ± 0.2
K_3PO4	10.8 ± 0.3	10.0 ± 0.3	11.7 ± 0.4	11.6 ± 0.3	12.3 ± 0.4	12.2 ± 0.2
K_2HPO_4	7.8 ± 0.3	7.2 ± 0.2	8.7 ± 0.2	8.2 ± 0.2	9.1 ± 0.2	8.7 ± 0.2
Na_2SO_3	7.9 ± 0.2	3.3 ± 0.1	8.6 ± 0.1	2.7 ± 0.1	8.6 ± 0.1	7.1 ± 0.3

NOM

	11.6 mg/L-TOC		23.1 mg/L-TOC		61.7 mg/L-TOC		123.4 mg/L-TOC	
	$pH_{initial}$	pH_{final}	$pH_{initial}$	pH_{final}	$pH_{initial}$	pH_{final}	$pH_{initial}$	pH_{final}
NOM	3.6 ± 0.2	2.7 ± 0.2	3.7 ± 0.3	2.7 ± 0.1	4.0 ± 0.4	2.9 ± 0.2	4.3 ± 0.2	3.0 ± 0.1

oxidation.

$$SO_4^{\bullet-} + HCO_3^- = SO_4^{2-} + HCO_3^{\bullet} \quad k = 9.1 \times 10^6\ M^{-1}\ s^{-1} \tag{11}$$

Impacts of PO_4^{3-} on reaction kinetics

PO_4^{3-} significantly ($p < 0.05$) promoted phenol degradation and the promoting effect was enhanced with increasing PO_4^{3-} concentrations (Figure 5(a)). The k_{obs} of 1 mM, 10 mM and 100 mM of PO_4^{3-} were 1.6, 2.0 and 3.9, times higher than that of the control (Figure 2(a)). The phenol removal efficiency data corroborated the k_{obs} data (Figure 2(b)). Similar to CO_3^{2-}, the hydrolysis of PO_4^{3-} created a strong basic condition (Table 1). As discussed previously, basic pH significantly enhanced the rate of phenol degradation by PS. Higher PO_4^{3-} concentration resulted in higher solution pH and thus faster phenol removal. Although PO_4^{3-} scavenges $SO_4^{\bullet-}$ to form phosphate radical ($PO_4^{\bullet 2-}$) (Equation (12)), the rate of the reaction of $PO_4^{\bullet 2-}$ with phenoxide is relatively high ($5.9 \times 10^8\ M^{-1} \cdot s^{-1}$, Equation (13)) (Neta *et al.* 1988), which significantly offset negative effects of $SO_4^{\bullet-}$ scavenging. This also contributed to the increases in phenol degradation rate in the presence of PO_4^{3-}.

$$SO_4^{\bullet-} + PO_4^{3-} = SO_4^{2-} + PO_4^{\bullet 2-} \tag{12}$$

$$PO_4^{\bullet 2-} + C_6H_5O^- = PO_4^{3-} + C_6H_5O^{\bullet} \quad k = 5.9 \times 10^8\ M^{-1} \cdot s^{-1} \tag{13}$$

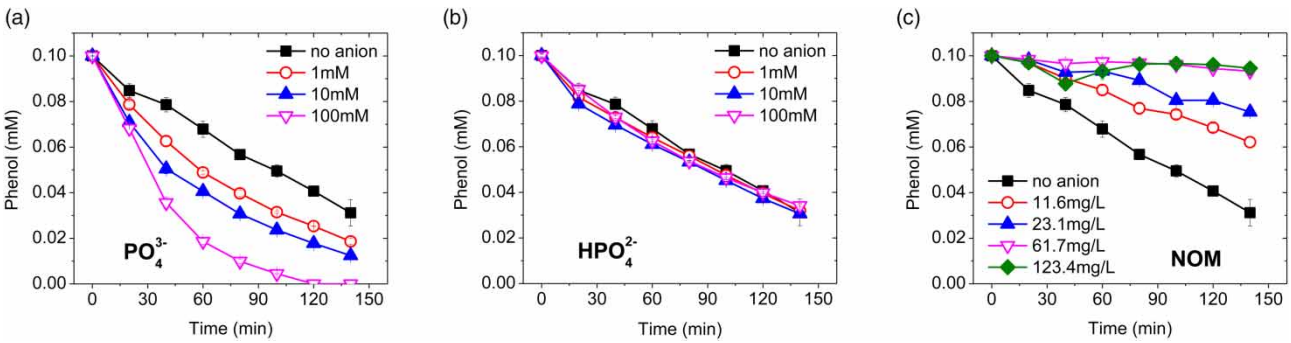

Figure 5 | Impacts of PO_4^{3-} (a), HPO_4^{2-} (b) and NOM (c) on phenol oxidation by TAP. Experimental conditions: $[PS]_0 = 10$ mM, [Phenol] = 0.1 mM, and T = 50 °C.

Impacts of HPO_4^{2-} on reaction kinetics

HPO_4^{2-} did not affect the PS oxidation of phenol. The phenol degradation plots 1–100 mM of HPO_4^{2-} almost overlapped with the plot of the no anion control (Figure 5(b)). Both k_{obs} data and the phenol removal efficiency data of 1–100 mM of HPO_4^{2-} had no statistically significant difference ($p > 0.05$) with those of the control (Figure 2). Several studies reported negligible influence of HPO_4^{2-} on PS-AOP (Yang *et al.* 2011; Nie *et al.* 2014). $SO_4^{\bullet-}$ can be scavenged by HPO_4^{2-} to produce $HPO_4^{\bullet-}$ (Equation (14)). The negligible influence of HPO_4^{2-} may be due to the relatively high reactivity of $HPO_4^{\bullet-}$ with phenol.

$$SO_4^{\bullet-} + HPO_4^{2-} = SO_4^{2-} + HPO_4^{\bullet-} \quad (14)$$

Impacts of NOM on reaction kinetics

The treatment containing higher concentrations of NOM had significantly lower ($p < 0.05$) phenol degradation rate and significantly lower ($p < 0.05$) phenol removal efficiency (Figures 2 and 5(c)). Electrophilic radicals such as $SO_4^{\bullet-}$ can easily attack the electron-rich moieties within NOM molecular structure (Equation (15)). Such reaction consumes reactive $SO_4^{\bullet-}$ and reduces the overall oxidation potential. Higher concentration of NOM leads to more $SO_4^{\bullet-}$ scavenged and lower PS oxidation rate. The inhibitory impacts of NOM on SR-AOP have also been reported by many studies (Nie *et al.* 2014; Jiang *et al.* 2016; Luo *et al.* 2016; Oliveira *et al.* 2016; Ferreira *et al.* 2017; Ma *et al.* 2018).

$$SO_4^{\bullet-} + NOM = products^- \quad k = 6.8 \times 10^3\ L\,mg - C^{-1}\,s^{-1} \quad (15)$$

Formation of undesired degradation byproducts and the proposed reaction pathways

In the control treatment without anions, six intermediates were identified: *p*-benzoquinone, 2-phenoxy-phenol, 4-phenoxy-phenol, 2,2′-dihydroxybiphenyl, 3,3′-dihydroxybiphenyl, and 4,4′-dihydroxybiphenyl (Table 2). Based on the above intermediates identified and the data from previous studies (Anipsitakis *et al.* 2006), the possible reaction pathway of PS oxidation of phenol is proposed as follows. The first step is the addition of a $SO_4^{\bullet-}$ to the aromatic ring, which results in an unstable form (P1) (Figure 6(a)). Since sulfate is an excellent leaving group, the hydroxycyclohexadienyl radical (P2) is formed via elimination of the sulfate group. Hydrolysis of the hydroxycyclohexadienyl radical (P2) leads to the formation of hydroxylated radical products, which further react with O_2 to form the stable intermediate hydroquinone (P3) (Anipsitakis *et al.* 2006). Quinone (P4) is then generated via hydrogen abstraction from hydroquinone (P3). Two hydroxycyclohexadienyl radicals (P2) may also combine with each other to generate dihydroxybiphenyls (P5, P6, and P7). An alternative pathway for the first step is that $SO_4^{\bullet-}$ reacts with phenol to form hydroxylated radicals (P8) via H abstraction. A hydroxylated radical may react with a hydroxycyclohexadienyl radical to form phenoxy-phenols (P9 and P10).

In the treatment containing Cl^-, GC-MS detected three chlorinated intermediates (2-chlorophenol, 4-chlorophenol,

Table 2 | Degradation intermediates identified in the control without anions and in the treatments containing halides[a]

PS + phenol	PS + phenol + Cl^-	PS + phenol + Br^-
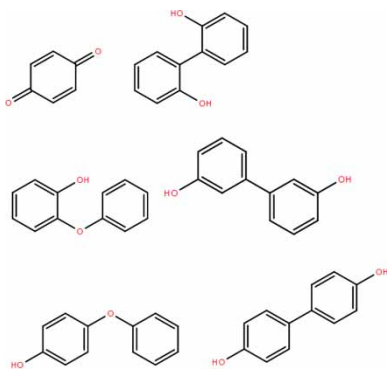	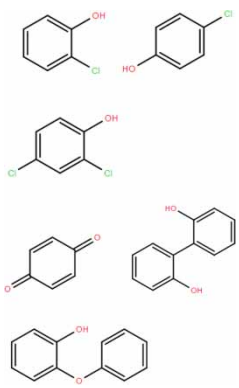	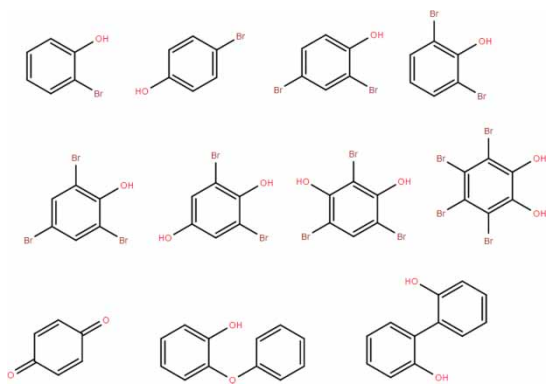

[a]The GC-MS spectrum for each halogenated intermediate can be found in the supplementary materials (available with the online version of this paper).

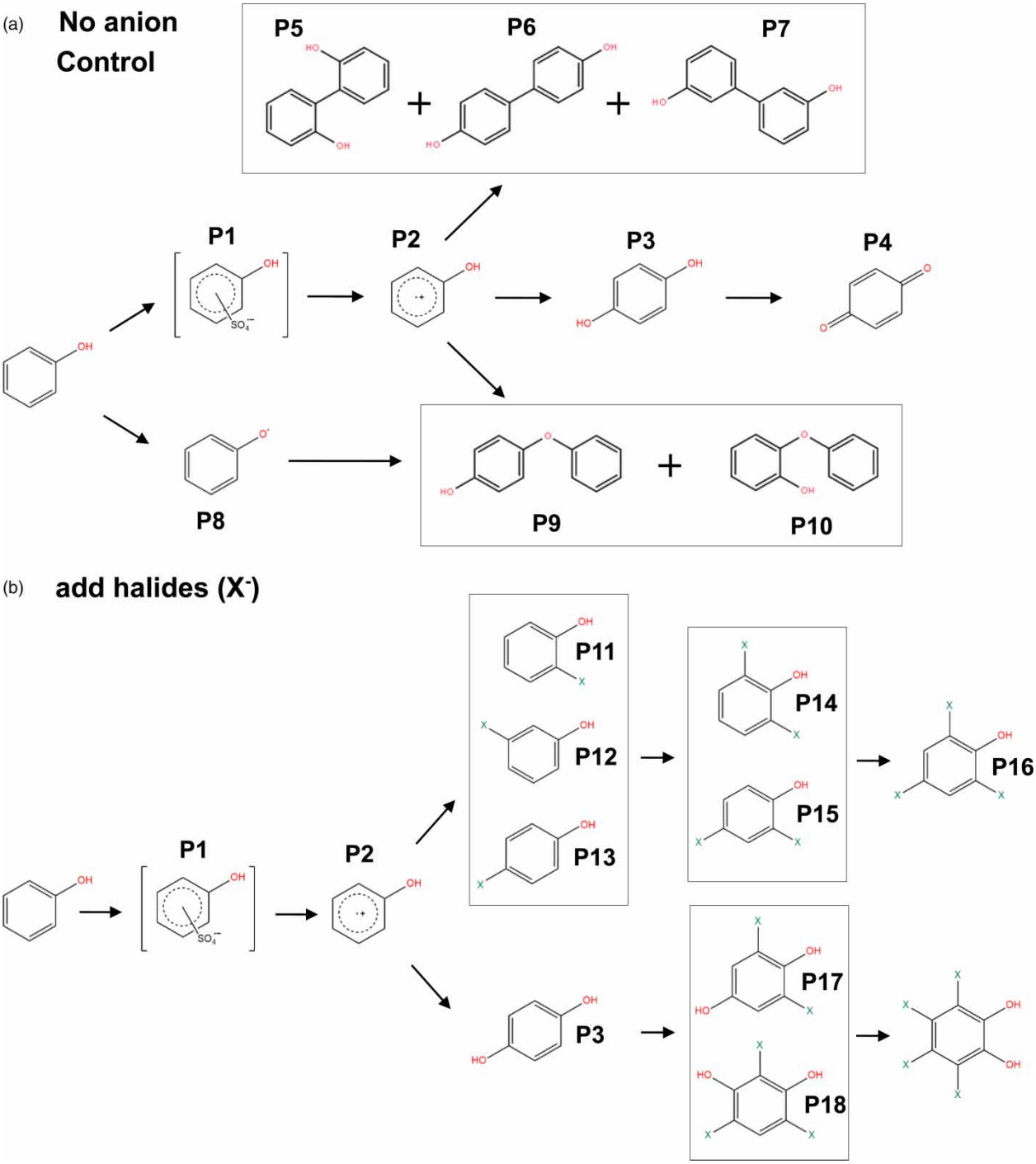

Figure 6 | Reaction pathway in the control treatment without anions (a) and in the treatment containing halides (b).

and 2, 4-dichlorophenol) and three non-halogen intermediates (*p*-benzoquinone, 2-phenoxy-phenol and 2,2′-dihydroxybiphenyl) (Table 2). In the treatment containing Br^-, GC-MS detected eight brominated intermediates (2-bromophenol, 4-bromophenol 2,4-dibromophenol, 2,6-dibromophenol, 2,4,6-tribromophenol, 2,6-dibromohydroquinone, 2,4,6-tribromo-1,3-benzenediol, and tetrabromocatechol) and the same three non-halogen intermediates as in the treatment containing Cl^- (Table 2). As discussed previously, Cl^- and Br^- can be oxidized by $SO_4^{\bullet-}$ through a series of chain reactions to

generate reactive halogen radicals (e.g., $X^{\bullet}$, $X_2^{\bullet-}$, and $XOH^{\bullet-}$). Given the relatively high concentration of Cl^- and Br^-, a significant fraction of $SO_4^{\bullet-}$ in the reaction solution was expected to be transformed to halogen radicals. It was reported that the concentration of generated halogen radicals could exceed that of $SO_4^{\bullet-}$ by several orders of magnitude (Yang *et al.* 2014). Halogen radicals are selective oxidants that can be involved in H abstraction, electron transfer, or addition reactions with organic compounds. It is generally accepted that H abstraction and electron transfer contribute to the mineralization of contaminants, whereas addition reaction leads to the formation of halogenated compounds. As previously discussed, $SO_4^{\bullet-}$ can attack the aromatic ring of phenol to form an unstable intermediate P1, which is then transformed to a hydroxycyclohexadienyl radical (P2) via elimination of the sulfate group (Figure 6(b)). The combination of a halogen radical with a hydroxycyclohexadienyl radical leads to the formation of monohalogenated byproducts (P11, P12 and P13). Further halogenation leads to the formation of dihalogenated byproducts (P14 and P15) and trihalogenated byproducts (P16) (Anipsitakis *et al.* 2006; Liu *et al.* 2015). An alternative pathway is that the hydrolysis of the hydroxycyclohexadienyl radical (P2) leads to the formation of hydroxylated radical products which further react with O_2 to form the stable intermediate hydroquinone (P3). Hydroquinone (P3) could react with halogen radicals to form halogenated hydroquinones (P17, P18, and P19). Formation of halogenated intermediates during SR-AOP oxidation of organic contaminants other than phenol have also been reported by other studies (Wang *et al.* 2014; Liu *et al.* 2015; Lu *et al.* 2015).

As discussed previously, reaction of $SO_4^{\bullet-}$ with anions other than halides may also generate secondary radicals such as $NO_3^{\bullet}$, $CO_3^{\bullet-}$, $HCO_3^{\bullet}$, $PO_4^{\bullet 2-}$, and $HPO_4^{\bullet-}$. Theoretically, these secondary radicals may also be involved in the radical chain propagation, thus influencing the byproduct distribution (Ji *et al.* 2017). Ji *et al.* found that nitrobenzene oxidation by heat-activated PS generated a series of byproducts including mononitrophenols, dinitrophenols, trinitrophenols, and coupling products (Ji *et al.* 2017). Formation of nitrated byproducts indicates that both denitration and renitration processes occur during PS oxidation of nitrobenzene. However, in this study, no new intermediates were identified in the treatment containing CO_3^{2-}, HCO_3^-, PO_4^{3-}, HPO_4^{2-}, and NO_3^- except for those intermediates detected in the no anion control. We acknowledge that absence of evidence is not evidence of absence. Therefore, further studies using more advanced analytical tools (e.g., high resolution mass spectrometer) are needed to have a better understanding of this problem.

CONCLUSION

This is the first study that has a comprehensive investigation on the impacts of eight anions (CO_3^{2-}, HCO_3^-, Cl^-, Br^-, PO_4^{3-}, HPO_4^{2-}, NO_3^-, and SO_3^{2-}) and NOM on the reaction kinetics and the formation of undesired degradation byproducts during phenol oxidation by SR-AOP. We found that different matrix species have different impacts on the kinetics of phenol oxidation by heat-activated PS. CO_3^{2-}, PO_4^{3-}, and Br^- promoted the reaction and the promoting effects were enhanced with increasing anion concentrations. NOM inhibited the reaction and the inhibiting effect was enhanced with increasing NOM concentrations. SO_3^{2-} with concentrations higher than 10 mM completely suppressed the reaction. HCO_3^-, Cl^-, NO_3^- and HPO_4^{2-} with the concentrations of 1–100 mM did not affect the reaction. In addition to the kinetic study, formation of degradation byproducts in the no anion control treatment and in the treatment containing CO_3^{2-}, HCO_3^-, Cl^-, Br^-, PO_4^{3-}, HPO_4^{2-}, and NO_3^- were screened by GC-MS. Six intermediates were detected in the no anion control (p-benzoquinone, 2-phenoxy-phenol, 4-phenoxy-phenol, 2,2′-dihydroxybiphenyl, 3,3′-dihydroxybiphenyl, and 4,4′-dihydroxybiphenyl). A variety of toxic halogenated phenols and hydroquinones were detected in the treatment containing Cl^- and Br^-. However, in the treatment containing CO_3^{2-}, HCO_3^-, PO_4^{3-}, HPO_4^{2-}, and NO_3^-, no new intermediates were identified except for the intermediates already detected in the no anion control. Based on the intermediates identified, reaction pathways for PS oxidation of phenol without anions and in the presence of halides were proposed respectively. Overall, we found that phenol can be effectively removed by heat-activated persulfate, but water matrix species significantly affected the reaction kinetics and may even produce halogenated byproducts. Because many halogenated organic compounds are toxic and/or refractory, great attention should be paid when SR-AOPs are used for wastewater treatment or soil and groundwater remediation when there are high levels of halides.

ACKNOWLEDGEMENTS

This study was financially supported by Beijing NOVA program (Grant No. Z181100006218088), Science Foundation of China University of Petroleum-Beijing (Grant No. 2462018BJC003), and the Independent Project Program of State Key Laboratory of Petroleum Pollution Control

(Grant No. PPCIP2017004), CNPC Research Institute of Safety & Environment Technology.

REFERENCES

Ahmad, M., Teel, A. L. & Watts, R. J. 2013 Mechanism of persulfate activation by phenols. *Environmental Science & Technology* **47** (11), 5864–5871.

Anipsitakis, G. P., Dionysiou, D. D. & Gonzalez, M. A. 2006 Cobalt-mediated activation of peroxymonosulfate and sulfate radical attack on phenolic compounds. Implications of chloride ions. *Environmental Science & Technology* **40** (3), 1000–1007.

Bennedsen, L. R., Muff, J. & Søgaard, E. G. 2012 Influence of chloride and carbonates on the reactivity of activated persulfate. *Chemosphere* **86** (11), 1092–1097.

De Luca, A., He, X., Dionysiou, D. D., Dantas, R. F. & Esplugas, S. 2017 Effects of bromide on the degradation of organic contaminants with UV and Fe^{2+} activated persulfate. *Chemical Engineering Journal* **318**, 206–213.

Ferreira, I. D., Prieto, T., Freitas, J. G., Thomson, N. R., Nantes, I. L. & Bechara, E. J. H. 2017 Natural persulfate activation for anthracene remediation in tropical environments. *Water Air and Soil Pollution* **228** (4), 146.

Furman, O. S., Teel, A. L. & Watts, R. J. 2010 Mechanism of base activation of persulfate. *Environmental Science & Technology* **44** (16), 6423–6428.

He, X., de la Cruz, A. A., O'Shea, K. E. & Dionysiou, D. D. 2014 Kinetics and mechanisms of cylindrospermopsin destruction by sulfate radical-based advanced oxidation processes. *Water Research* **63**, 168–178.

Hu, P. & Long, M. 2016 Cobalt-catalyzed sulfate radical-based advanced oxidation: a review on heterogeneous catalysts and applications. *Applied Catalysis B: Environmental* **181**, 103–117.

Ji, Y., Shi, Y., Wang, L. & Lu, J. 2017 Denitration and renitration processes in sulfate radical-mediated degradation of nitrobenzene. *Chemical Engineering Journal* **315**, 591–597.

Jiang, C., Ji, Y., Shi, Y., Chen, J. & Cai, T. 2016 Sulfate radical-based oxidation of fluoroquinolone antibiotics: kinetics, mechanisms and effects of natural water matrices. *Water Research* **106**, 507–517.

Liu, K., Lu, J. & Ji, Y. 2015 Formation of brominated disinfection by-products and bromate in cobalt catalyzed peroxymonosulfate oxidation of phenol. *Water Research* **84**, 1–7.

Lu, J., Wu, J., Ji, Y. & Kong, D. 2015 Transformation of bromide in thermo activated persulfate oxidation processes. *Water Research* **78**, 1–8.

Luo, C., Jiang, J., Ma, J., Pang, S., Liu, Y., Song, Y., Guan, C., Li, J., Jin, Y. & Wu, D. 2016 Oxidation of the odorous compound 2,4,6-trichloroanisole by UV activated persulfate: kinetics, products, and pathways. *Water Research* **96**, 12–21.

Ma, J., Li, H., Chi, L., Chen, H. & Chen, C. 2017 Changes in activation energy and kinetics of heat-activated persulfate oxidation of phenol in response to changes in pH and temperature. *Chemosphere* **189**, 86–93.

Ma, J., Yang, Y., Jiang, X., Xie, Z., Li, X., Chen, C. & Chen, H. 2018 Impacts of inorganic anions and natural organic matter on thermally activated persulfate oxidation of BTEX in water. *Chemosphere* **190**, 296–306.

Neta, P., Huie, R. E. & Ross, A. B. 1988 Rate constants for reactions of inorganic radicals in aqueous solution. *Journal of Physical and Chemical Reference Data* **17** (3), 1027–1284.

Nie, M., Yang, Y., Zhang, Z., Yan, C., Wang, X., Li, H. & Dong, W. 2014 Degradation of chloramphenicol by thermally activated persulfate in aqueous solution. *Chemical Engineering Journal* **246**, 373–382.

Oliveira, F. C., Freitas, J. G., Furquim, S. A. C., Rollo, R. M., Thomson, N. R., Alleoni, L. R. F. & Nascimento, C. A. O. 2016 Persulfate interaction with tropical soils. *Water Air and Soil Pollution* **227** (9), 343.

Sun, H. & Wang, S. 2015 Catalytic oxidation of organic pollutants in aqueous solution using sulfate radicals. In: *Catalysis: Specialist Periodical Reports* (J. Spivey & Y.-F. Han, eds). The Royal Society of Chemistry, UK, pp. 209–247.

Wang, Z., Yuan, R., Guo, Y., Xu, L. & Liu, J. 2011 Effects of chloride ions on bleaching of azo dyes by Co^{2+}/oxone regent: kinetic analysis. *Journal of Hazardous Materials* **190** (1–3), 1083–1087.

Wang, Y. R., Le Roux, J., Zhang, T. & Croue, J. P. 2014 Formation of brominated disinfection byproducts from natural organic matter isolates and model compounds in a sulfate radical-based oxidation process. *Environmental Science & Technology* **48** (24), 14534–14542.

Yang, S., Wang, P., Yang, X., Shan, L., Zhang, W., Shao, X. & Niu, R. 2010 Degradation efficiencies of azo dye Acid Orange 7 by the interaction of heat, UV and anions with common oxidants: persulfate, peroxymonosulfate and hydrogen peroxide. *Journal of Hazardous Materials* **179** (1–3), 552–558.

Yang, S., Yang, X., Shao, X., Niu, R. & Wang, L. 2011 Activated carbon catalyzed persulfate oxidation of Azo dye acid orange 7 at ambient temperature. *Journal of Hazardous Materials* **186** (1), 659–666.

Yang, Y., Pignatello, J. J., Ma, J. & Mitch, W. A. 2014 Comparison of halide impacts on the efficiency of contaminant degradation by sulfate and hydroxyl radical-based advanced oxidation processes (AOPs). *Environmental Science & Technology* **48** (4), 2344–2351.

Yang, J.-F., Yang, L.-M., Zhang, S.-B., Ou, L.-H., Liu, C.-B., Zheng, L.-Y., Yang, Y.-F., Ying, G.-G. & Luo, S.-L. 2017 Degradation of azole fungicide fluconazole in aqueous solution by thermally activated persulfate. *Chemical Engineering Journal* **321**, 113–122.

Zhang, B.-T., Zhang, Y., Teng, Y. & Fan, M. 2015 Sulfate radical and its application in decontamination technologies. *Critical Reviews in Environmental Science and Technology* **45** (16), 1756–1800.

First received 22 December 2017; accepted in revised form 19 March 2018. Available online 2 April 2018